Circulation Journal
Official Journal of the Japanese Circulation Society
http://www.j-circ.or.jp

ORIGINAL ARTICLE
Imaging

Accuracy of Optical Frequency Domain Imaging for Evaluation of Coronary Adventitial Vasa Vasorum Formation After Stent Implantation in Pigs and Humans

– A Validation Study –

Kensuke Nishimiya, MD, PhD; Yasuharu Matsumoto, MD, PhD; Hironori Uzuka, MD; Kazuma Oyama, MD; Atsushi Tanaka, MD, PhD; Akira Taruya, MD; Tsuyoshi Ogata, MD; Michinori Hirano, MD; Tomohiko Shindo, MD; Kenichiro Hanawa, MD, PhD; Yuhi Hasebe, MD, PhD; Kiyotaka Hao, MD, PhD; Ryuji Tsuburaya, MD, PhD; Jun Takahashi, MD, PhD; Satoshi Miyata, PhD; Kenta Ito, MD, PhD; Takashi Akasaka, MD, PhD; Hiroaki Shimokawa, MD, PhD

Background: Coronary adventitia harbors a wide variety of components, such as inflammatory cells and vasa vasorum (VV). Adventitial VV initiates the development of coronary artery diseases as an outside-in supply route of inflammation. We have recently demonstrated that drug-eluting stent implantation causes the enhancement of VV formation, with extending to the stent edges in the porcine coronary arteries, and also that optical frequency domain imaging (OFDI) is capable of visualizing VV in humans in vivo. However, it remains to be fully validated whether OFDI enables the precise measurement of VV formation in pigs and humans.

Methods and Results: In the pig protocol, a total of 6 bare-metal stents and 12 drug-eluting stents were implanted into the coronary arteries, and at 1 month, the stented coronary arteries were imaged by OFDI ex vivo. OFDI data including the measurement of VV area at the stent edge portions were compared with histological data. There was a significant positive correlation between VV area on OFDI and that on histology ($R=0.91$, $P<0.01$). In the human protocol, OFDI enabled the measurement of the VV area at the stent edges after coronary stent implantation in vivo.

Conclusions: These results provide the first direct evidence that OFDI enables the precise measurement of the VV area in coronary arteries after stent implantation in pigs and humans. (*Circ J* 2015; **79:** 1323–1331)

Key Words: Drug-eluting stents; Imaging; Inflammation; Optical coherence tomography

Coronary adventitia harbors a large variety of components such as inflammatory cells/cytokines[1–5] and nutrient blood vessels of the vascular wall, which is termed vasa vasorum (VV).[6,7] Particularly, adventitial VV precedes the development of coronary atherosclerotic lesions[8] and plays a key role as an outside-in supply route of vascular inflammation.[4] We have recently demonstrated that adventitial VV formation is dramatically increased in the porcine coronary arteries after drug-eluting stent (DES) implantation with extending to the stent edge portions, associated with coronary hyperconstricting responses.[9] Thus, adventitial VV has been proposed as a novel therapeutic target for coronary artery diseases (CAD).[10,11]

In order to better understand the pathophysiological role of adventitial VV in patients with CAD, advanced imaging for coronary adventitial VV is warranted. We have recently demonstrated that optical frequency domain imaging (OFDI), which has been developed as a newer-generation optical coherence tomography (OCT) with excellent sensitivity,[12–14] is capable of clearly visualizing adventitial VV in human coronary lesions in vivo.[15] However, it remains to be validated whether the OFDI system enables us to accurately measure coronary adventitial VV area in animals and humans.

Editorial p1211

Received January 20, 2015; revised manuscript received February 19, 2015; accepted February 20, 2015; released online April 3, 2015
Time for primary review: 14 days

Department of Cardiovascular Medicine, Tohoku University Graduate School of Medicine, Sendai (K.N., Y.M., H.U., K.O., T.O., M.H., T.S., K. Hanawa, Y.H., K. Hao, R.T., J.T., S.M., K.I., H.S.); Department of Cardiovascular Medicine, Wakayama Medical University, Wakayama (A. Tanaka, A. Taruya, T.A.), Japan

The Guest Editor for this article was Ken-ichi Hirata, MD.

Mailing address: Yasuharu Matsumoto, MD, PhD, Department of Cardiovascular Medicine, Tohoku University Graduate School of Medicine, 1-1 Seiryo-machi, Aoba-ku, Sendai 980-8574, Japan. E-mail: matsumoto@cardio.med.tohoku.ac.jp

ISSN-1346-9843 doi:10.1253/circj.CJ-15-0078

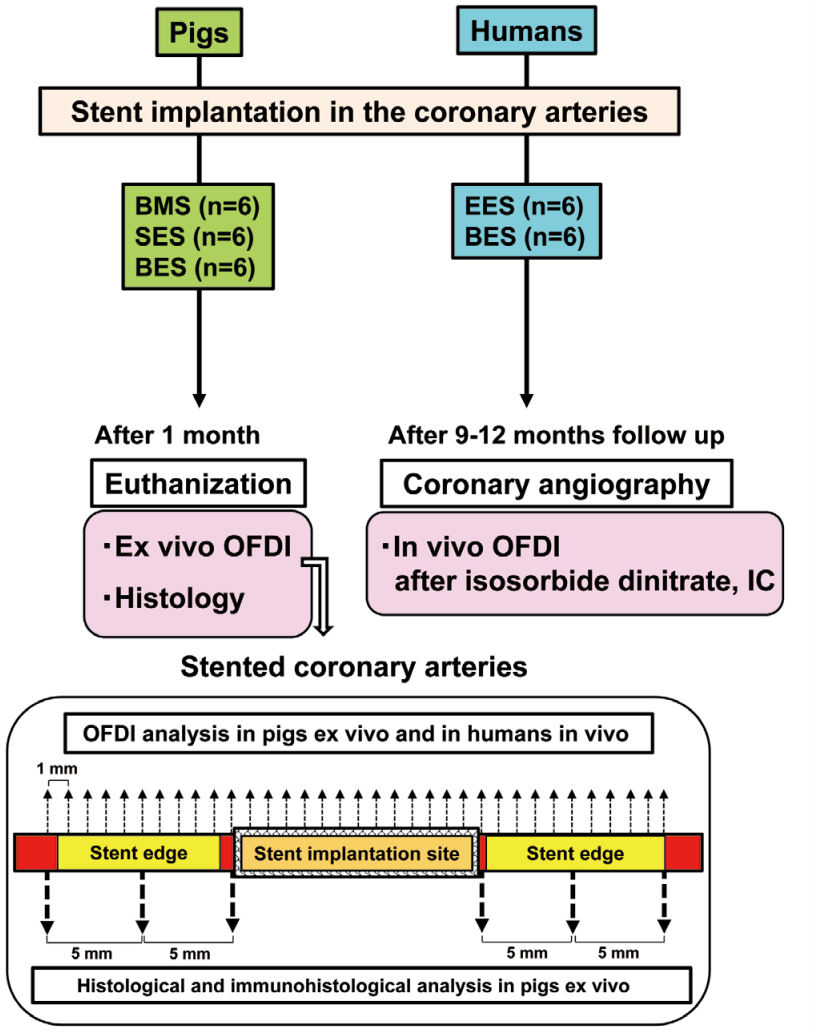

Figure 1. Study protocol. In the pig protocol, bare-metal stents (BMS), sirolimus-eluting stents (SES) and biolimus A9-eluting stents (BES) (n=6 each) were randomly implanted into the left porcine coronary arteries. After euthanization at 1 month, the cross-sectional optical frequency domain imaging (OFDI) at every 1 mm length and the histology of the stent edges at 3 different cross-sections in the proximal and distal stent edges, including those adjacent to and 5 and 10 mm apart from the stent, were obtained. OFDI data including the adventitial vasa vasorum (VV) area on OFDI were then correlated with those in histology sections. In the human protocol, patients who had undergone coronary stent implantation were imaged by OFDI after intracoronary administration of isosorbide dinitrate.

In the present study, we thus examined whether OFDI is a useful tool for precisely measuring coronary adventitial VV area in pigs and humans.

Methods

All animal care and experiments were performed in accordance with the Guide for the Care and Use of Laboratory Animals published by the U.S. National Institute of Health (NIH Publication, 8th Edition, 2011), and were approved by the Institutional Committee for Use of Laboratory Animals of Tohoku University (2013MdA-059). All protocols using human samples were approved by the ethics committee of Tohoku University Graduate School of Medicine (2014-1-640).

Study Protocols

The present study consisted of the pig and human protocols. In the pig protocol, we performed OFDI measurement of coronary adventitial VV at 1 month after DES implantation ex vivo and compared the OFDI data with histological data. In the human protocol, we examined whether the OFDI system enables us to evaluate adventitial VV in patients with DES implantation in vivo.

Animal Preparation

Nine Göttingen miniature pigs (male, 1 year old and weighing 25–30 kg) were pre-treated orally with aspirin (200 mg/day) and clopidogrel (225 mg/day) for 2 days before stent implantation. After sedation with medetomidine (0.1 mg/kg, IM) and midazolam (0.2 mg/kg, IM), followed by inhaled sevoflurane (2–5%) and heparinization (5,000 U, IV), we randomly implanted bare-metal stents (BMS) (Terumo Corporation, Tokyo, Japan), sirolimus-eluting stents (SES) (Cypher Select; Johnson & Johnson, New Brunswick, NJ, USA) and biolimus A9-eluting stents (BES) (Nobori, Terumo Corporation, Tokyo, Japan) (n=6, each) into the left anterior descending and the left circumflex coronary arteries in the same pig (n=9) for the histological validation study (Figure 1).[16,17] The balloon inflation ratio was adjusted to achieve an overstretch ratio of 1.0–1.1 under the guidance of intravascular ultrasound (View IT; Terumo Corporation, Tokyo, Japan).[16–18] There was no significant difference in the stent implantation procedure among the 3 groups (Table S1). A quantitative coronary angiography for stent implantation procedures was performed by 2 independent investigators (K.N. and H.U.). The anti-platelet therapy with oral aspirin (100 mg/day) and clopidogrel (75 mg/day) was continued until euthanasia.

Acquisition of OFDI in Pigs

At 1 month after stent implantation, the animals were euthanized with a lethal dose of sodium pentobarbital (40 mg/kg, IV) after deep sedation with 5% inhaled sevoflurane; the heart was then gently removed (n=6 each) (Figure 1). Subsequently, saline and 10% neutral buffered formalin were immediately infused into the left coronary arteries via a constant perfusion pressure system (120 cm H_2O).[16,17] The harvested heart was then fixed with 10% neutral buffered formalin for 24 h. After the whole-heart sample preparation, we performed the OFDI imaging (LUNAWAVE; Terumo, Tokyo, Japan). We introduced an OFDI catheter (Fast View; Terumo, Tokyo, Japan) into the stented left coronary artery with the introduction of an intracoronary guide-wire, and then performed serial OFDI acquisition, with an automatic pullback rate of 40 mm/s.

Morphometric Analysis and OFDI Measurement of Coronary Adventitial VV

Morphometric analysis on OFDI was performed independently by 2 investigators (K.N. and H.U.). At every 1 mm length of the cross-sectional OFDI images, morphometric parameters were manually measured by using Image J (U.S. National Institute of Health, Bethesda, Maryland) (Figure 1). In the stent sites, the neointimal area was calculated by the following formula: [stent area–lumen area]; and Area stenosis was calculated as: 100×[1–(lumen area/stent area)] (Figure 2).[18] Because it was difficult to observe the adventitial area due to attenuation of stent struts in the stent sites, the cross-sectional OFDI images were used for the measurement of the coronary adventitial VV area. In the stent edges, the adventitial area was calculated by the following formula: [Area outside the external elastic lamina (EEL) within a distance of the thickness of the intima plus media–EEL area], as previously described.[19,20] Adventitial VV was defined as signal-voiding tubular structures that were sharply identified on more than 3 consecutive cross-sectional OFDI images, as previously described.[21] The adventitial VV area was manually traced in the adventitial area.

Preparations of Histological Sections

Following coronary artery interrogation with OFDI, the proximal and distal stent edge portions of the stented vessels were isolated for histological and immunohistological analyses. At 3 different cross-sections in the proximal and distal stent edges, including adjacent to and 5 and 10 mm apart from the stent, coronary arteries with perivascular tissues were gently separated for the paraffin sections, and were cut into a 3 μm-thick slices (Figure 1). All sections of the stent edges were stained with Masson's trichrome, rabbit anti-human von Willebrand factor (vWF) antibody (1:3) (N1505; Dako, Copenhagen, Denmark) for VV, mouse anti-human smooth muscle actin clone 1A4 (α-SMA) antibody (1:200) (ab7817; Abcam, Cambridge, UK) for smooth muscle actin and appropriate non-immune IgG. A total of 48 sections were excluded for the basis of cutting artifacts, co-registration difficulty and large branch. Finally, morphometric parameters of 60 histological sections of the stent edges were correlated with the OFDI images.

Histomorphometric Analysis and Measurement of Coronary Adventitial VV

Histomorphometric analysis was performed independently by 2 investigators (K.N. and H.U.). In the sections of the stent edges, histomorphometric parameters were manually measured by using Axio Vision (Carl Zeiss, Oberkochen, Germany). The adventitial area was defined as the area outside the EEL within a distance of the thickness of intima plus media, as previously described.[19,20] The vWF-positive luminal area (adventitial VV area) was manually traced in the adventitial area.

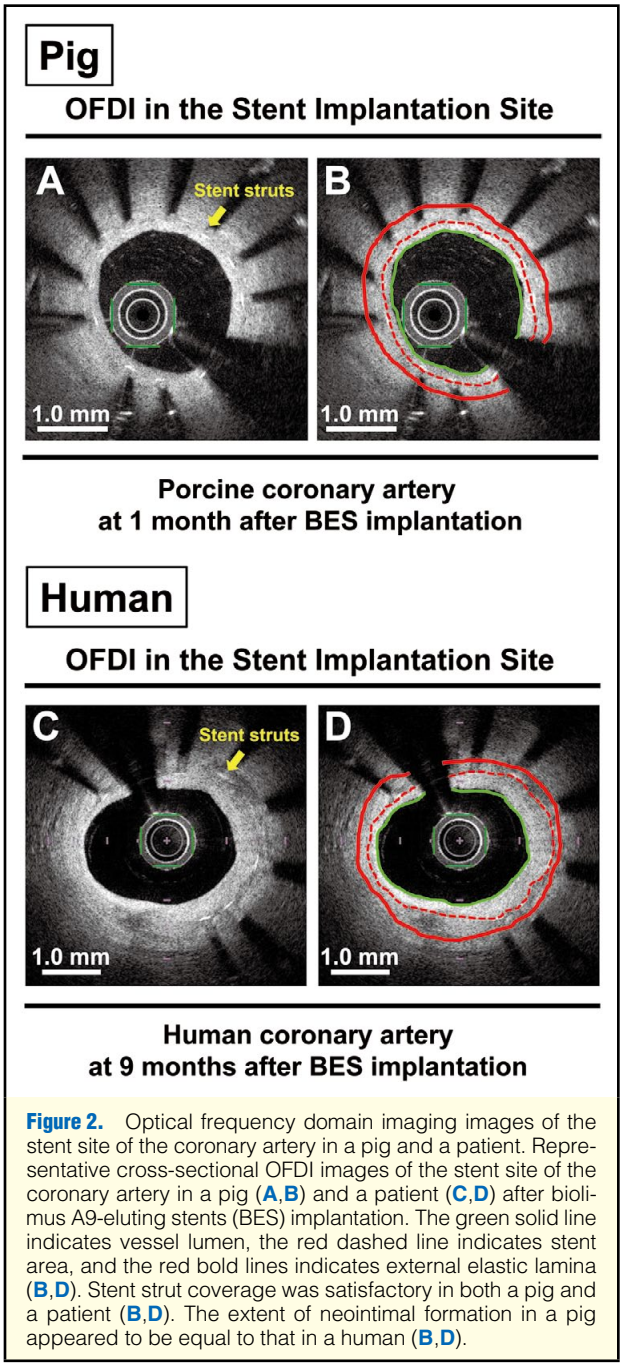

Figure 2. Optical frequency domain imaging images of the stent site of the coronary artery in a pig and a patient. Representative cross-sectional OFDI images of the stent site of the coronary artery in a pig (**A**,**B**) and a patient (**C**,**D**) after biolimus A9-eluting stents (BES) implantation. The green solid line indicates vessel lumen, the red dashed line indicates stent area, and the red bold lines indicates external elastic lamina (**B**,**D**). Stent strut coverage was satisfactory in both a pig and a patient (**B**,**D**). The extent of neointimal formation in a pig appeared to be equal to that in a human (**B**,**D**).

Histology/OFDI Coregistration in the Measurement of Coronary Adventitial VV

In the proximal and distal stent edges, the cross-sectional OFDI images were selected by using the pullback speed and frame numbers to match the pre-selected histology from 3 different cross-sections, including adjacent to, and 5 and 10 mm apart from the stent (Figure 1). A total of 60 cross-sections were finally matched, in which correlations between the morphometric parameters, including the adventitial VV area and those on OFDI, were analyzed.

Table 1. Morphometric Analysis of the Stent Sites With OFDI in Pigs

	Lumen diameter (mm)	Stent diameter (mm)	Neointimal thickness (mm)	Lumen area (mm^2)	Stent area (mm^2)	% area stenosis (%)
OFDI (n=264)	1.86±0.01	2.19±0.01	0.19±0.01	2.60±0.04	3.80±0.03	31.6±0.9
BMS (n=90)	1.69±0.03	2.17±0.02	0.22±0.02	2.25±0.08	3.57±0.05	36.8±2.1
SES (n=84)	1.90±0.02	2.25±0.02	0.15±0.01	2.95±0.05	4.09±0.05	27.9±1.0
BES (n=90)	1.81±0.02	2.16±0.02	0.18±0.01	2.63±0.06	3.76±0.06	29.9±1.2
P value	<0.01	<0.01	<0.01	<0.01	<0.01	<0.01
BMS vs. SES	<0.01	<0.01	<0.01	<0.01	<0.01	<0.01
BMS vs. BES	<0.01	0.95	0.07	<0.01	<0.05	<0.01
SES vs. BES	<0.05	<0.01	0.23	<0.01	<0.01	0.64

Results are expressed as mean±SEM. Percent area stenosis was calculated by using the following formula: 100×[1−(lumen area/stent area)]. OFDI, optical frequency domain imaging.

Table 2. Comparison of Morphometric Data of the Stent Edges Between Histology and OFDI in Pigs

	Lumen diameter (mm)	Intimal/medial thickness (mm)	Lumen area (mm^2)	EEL area (mm^2)	Adventitial area (mm^2)
Histology (n=60)	1.32±0.05	0.16±0.01	1.44±0.10	2.25±0.14	0.91±0.07
BMS (n=18)	1.14±0.05	0.17±0.02	1.04±0.10	1.76±0.19	0.77±0.09
SES (n=20)	1.34±0.09	0.17±0.02	1.55±0.17	2.47±0.28	0.98±0.13
BES (n=22)	1.45±0.09	0.15±0.01	1.65±0.19	2.45±0.24	0.97±0.11
P value	<0.05	0.62	<0.05	0.07	0.34
BMS vs. SES	0.22	0.98	0.09	0.10	0.39
BMS vs. BES	<0.05	0.63	0.03	0.11	0.41
SES vs. BES	0.57	0.74	0.90	1.00	1.00
OFDI (n=60)	1.24±0.04	0.22±0.01	1.33±0.11	2.32±0.15	1.29±0.08
BMS (n=18)	1.11±0.06	0.19±0.01	1.12±0.12	1.96±0.19	1.12±0.17
SES (n=20)	1.23±0.07	0.23±0.01	1.26±0.14	2.33±0.25	1.41±0.12
BES (n=22)	1.35±0.08	0.22±0.02	1.57±0.23	2.60±0.28	1.32±0.11
P value	0.07	0.18	0.20	0.22	0.32
BMS vs. SES	0.52	0.17	0.98	0.58	0.30
BMS vs. BES	0.06	0.41	0.19	0.19	0.55
SES vs. BES	0.43	0.81	0.24	0.72	0.87
Correlations					
R	0.77	0.67	0.75	0.81	0.68
P value	<0.0001	<0.0001	<0.0001	<0.0001	<0.0001

Results are expressed as mean±SEM. The adventitial area was calculated by using the following formula: [area outside EEL within a distance of the thickness of intima plus media−EEL area]. EEL, external elastic lamina.

Table 3. Morphometric Analysis of the Stent Sites With OFDI in Humans

	Lumen diameter (mm)	Stent diameter (mm)	Neointimal thickness (mm)	Lumen area (mm^2)	Stent area (mm^2)	% area stenosis (%)
OFDI (n=337)	2.96±0.04	3.05±0.03	0.13±0.01	6.69±0.11	8.15±0.12	17.9±0.6
EES (n=183)	2.59±0.03	2.87±0.03	0.13±0.01	6.95±0.13	7.56±0.16	18.7±0.6
BES (n=154)	3.39±0.08	3.28±0.03	0.14±0.02	7.39±0.17	8.90±0.15	16.9±1.2
P value	<0.0001	<0.0001	0.49	<0.0001	<0.0001	0.15

Results are expressed as mean±SEM. Percent area stenosis was calculated by using the following formula: 100×[1−(lumen area/stent area)].

OFDI Acquisition in Patients In Vivo

At 9–10 months after stent implantation, OFDI images of stented left coronary arteries were obtained in 12 patients without angiographic restenosis who had underwent stent implantation with an everolimus-eluting stent (EES) (Xience V; Abbot Vascular, Santa Clara, CA, USA; Promus, Boston Scietific, Marlborough, MA, USA) and BES (n=6 each) (**Figure 1**). Patient characteristics are described in **Table S2**. Initially, an intracoronary guidewire was introduced into the stented vessel followed by an OFDI catheter through a 6 Fr guiding catheter after intracoronary administration of isosorbide dinitrate (1–2 mg). Serial OFDI acquisition was then performed with an automatic pullback speed (40 mm/s) during an intracoronary injection of contrast medium mixed with an equivalent vol-

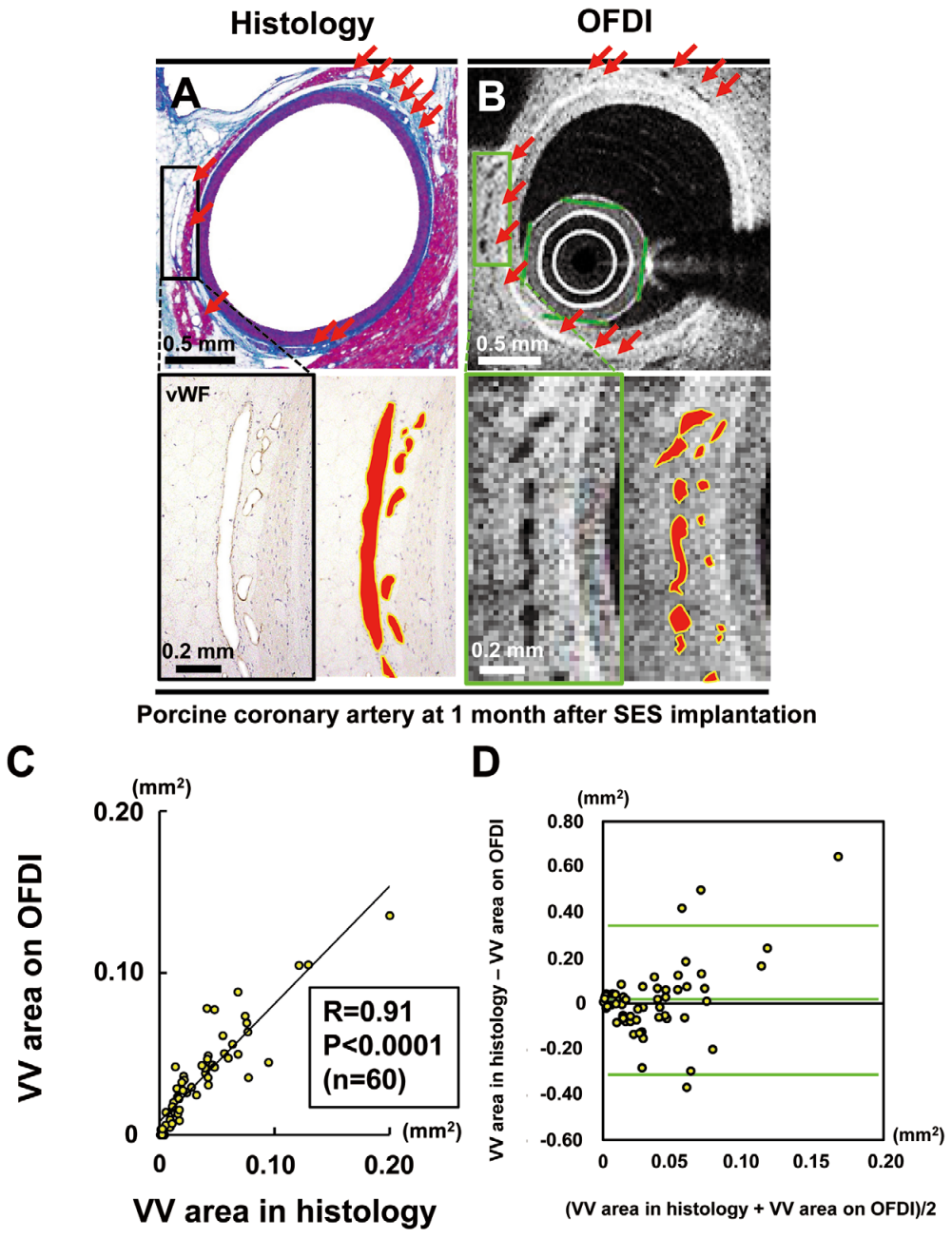

Figure 3. Histological validation for optical frequency domain imaging (OFDI) measurement of coronary adventitial vasa vasorum in pigs. Representative Masson's trichrome and von Willebrand factor (vWF) stainings (**A**) and cross-sectional OFDI image (**B**) of the stent edges of a porcine coronary artery after sirolimus-eluting stent (SES) implantation. The red arrows indicate microlumen structures in the coronary adventitia, which are positive for vWF, thus representing adventitial vasa vasorum (VV) (**A**). In the OFDI images, signal-voiding tubular structures in the coronary adventitia, indicated by red arrows, accurately correspond to adventitial VV in histology (**A**,**B**). The adventitial VV area manually traced in vWF staining and that on the OFDI image are shown by the red area (**A**,**B**). There is a significant positive correlation between adventitial VV area on OFDI and that in histology (**C**). The result of Bland-Altman analysis confirmed good agreements of the measurement of the adventitial VV area on OFDI with a marginal range of limits of agreement on OFDI (**D**).

ume of dextran. Detailed morphometric analysis was performed independently by 2 investigators (H.U. and K.O.). In the stent edges, in order to avoid the influence of vessel size, the adventitial VV area was calculated by the following formula: [VV area/adventitial area], as previously described.[19]

Statistical Analysis

Results are expressed as mean±standard error of the mean (SEM). Throughout the text and figures, n represents the number of sections. All histology and OFDI measurements were performed independently by 2 investigators. A comparison of

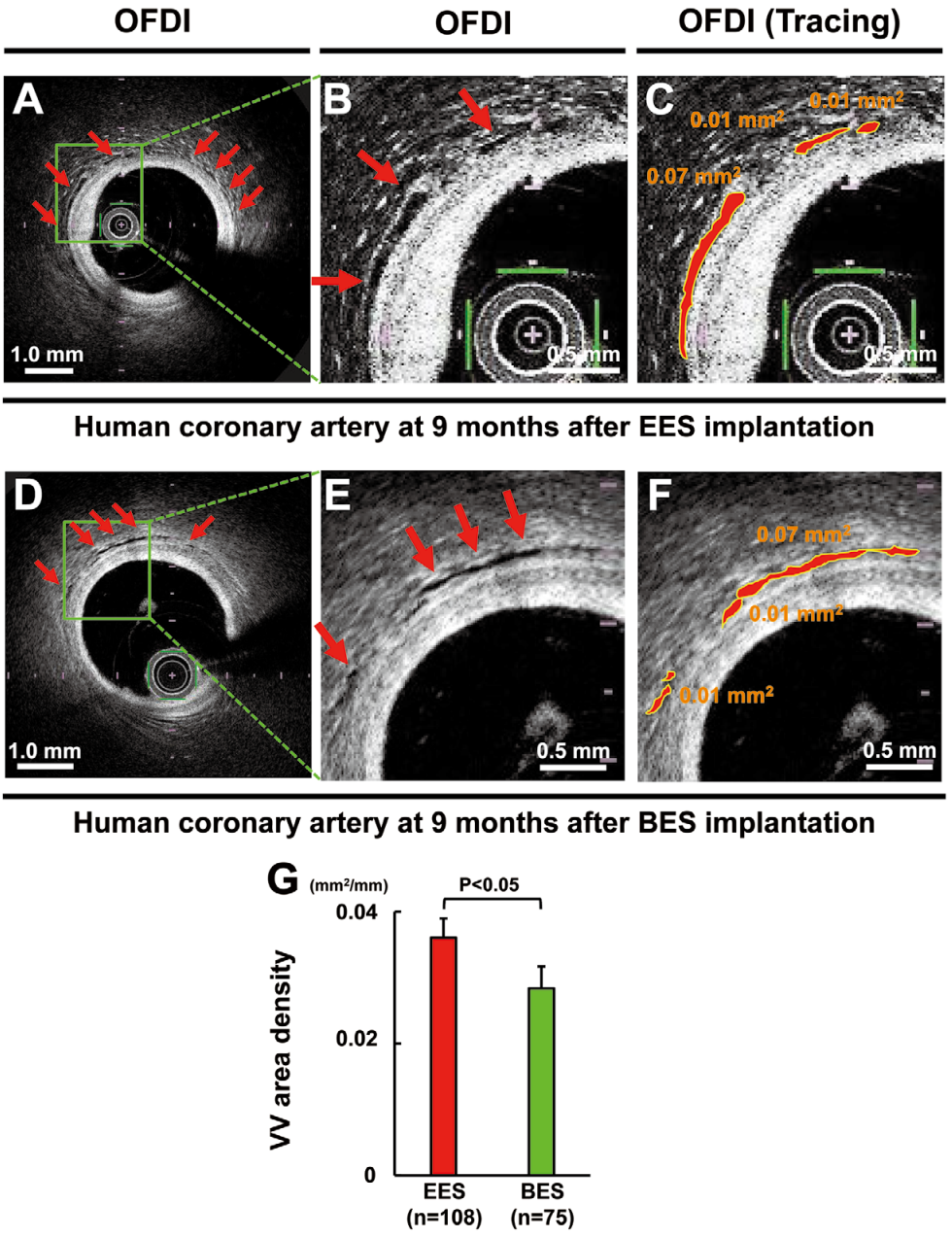

Figure 4. Coronary adventitial vasa vasorum (VV) on optical frequency domain imaging (OFDI) in patients with coronary artery disease. Representative cross-sectional OFDI images of the stent edges of human coronary arteries at 9 months after everolimus-eluting stent (EES) implantation in a 65-year-old male patient with angina pectoris (**A**–**C**) and biolimus A9-eluting stents (BES) implantation in a 68-year-old male patient with angina pectoris (**D**–**F**). The red arrows indicate adventitial VV as signal-voiding tubular structures in the coronary adventitia (**A**,**B**,**D**,**E**). The adventitial VV area on the OFDI image is shown by the red area, indicating that the OFDI system enables us to precisely measure coronary adventitial VV area in a human in vivo (**C**,**F**). The bar graph shows that adventitial VV area density was significantly greater at the EES site compared with the BES site (**G**). Error bar indicates mean±SEM.

the morphometric data was performed by one-way analysis of variance with the post-hoc Turkey-Kramer test in the pig protocol and by an unpaired, 2-sided Student's t-test or Mann-Whitney U-test in the human protocol. A correlation between continuous variables was analyzed using a linear regression model. Linear regression analyses were also performed for examining intra- and inter-observer variabilities in the present OFDI measurement, as previously described,[22] confirming the high reproducibility of the measurements (**Tables S3**,**S4**). The agreement of measurements was assessed by Bland-Altman analysis.[23] Statistical analysis was performed with IBM SPSS Statistics 20 software (IBM, New York, NY, USA). A P value

Table 4. Morphometric Analysis of the Stent Edges With OFDI in Humans

	Vasa vasorum area (mm^2)	Lumen diameter (mm)	Intimal/medial thickness (mm)	Lumen area (mm^2)	EEL area (mm^2)	Adventitial area (mm^2)
OFDI (n=183)	0.28±0.01	2.18±0.06	0.42±0.01	4.44±0.24	8.11±0.42	4.47±0.25
EES (n=108)	0.33±0.02	2.16±0.09	0.45±0.02	4.32±0.27	8.48±0.63	5.12±0.39
BES (n=75)	0.21±0.01	2.21±0.08	0.37±0.01	4.53±0.35	7.57±0.47	3.53±0.22
P value	<0.0001	0.65	<0.005	0.65	0.28	<0.005

Results are expressed as mean ± SEM. Adventitial area was calculated by using the following formula: [area outside EEL within a distance of the thickness of intima plus media−EEL area].

less than 0.05 was considered to be statistically significant.

Results

Morphometric Analysis on OFDI and in Histology in Pigs

The cross-sectional OFDI image of the BES site showed that stent strut was covered by the neointima, which was similar to the cross-sectional OFDI image of the BES site at 9 months in a patient (Figure 2). In the cross-sectional OFDI images of the stent sites, the % area stenosis in the BMS sites was significantly greater as compared with the SES and the BES sites (Table 1). In the cross-sectional OFDI images of the stent edges that corresponded to histological sections, morphometric parameters on OFDI were all comparable among the 3 stent sites (Table 2). Furthermore, there were significant positive correlations between OFDI and histology data (Table 2). In the human protocol, the morphometric analysis showed that the lumen and stent size of the BES site were significantly greater compared with the EES site, whereas the % area stenosis was comparable between the 2 stent sites (Table 3).

Histological Validation of the OFDI Measurement of Coronary Adventitial VV in Pigs

In the pig protocol, adventitial vessels positive for vWF (=VV) were partially negative for α-SMA staining, indicating that VV in histology consists of both arterial and venous vessels (Figures 3A,S1). The cross-sectional OFDI image at the SES site clearly visualized coronary adventitial VV as signal-voiding tubular structures (Figures 3A,B). Furthermore, the adventitial VV area manually traced on OFDI corresponded to that in the immunostaining for VV (Figures 3A,B). Adventitial VV formation was significantly diminished at the distal stent edges, 5 mm apart from the stents, as compared with the stent adjacent edge portions (Figure S2). Notably, there was a significant positive correlation between adventitial VV area on OFDI and that in histology (Figure 3C). Bland-Altman analysis confirmed good agreements of the measurement of adventitial VV area on OFDI, with a marginal range of limits of agreement on OFDI ([95% confidence interval (CI): –0.03 to 0.03μm^2) (Figure 3D). Similarly, in all cross-sectional OFDI images examined in the pig protocol, the adventitial VV area was significantly augmented in the SES site as compared with the BMS and BES sites (Table S5).

OFDI Measurement of Coronary Adventitial VV in Humans

In the human protocol, the cross-sectional OFDI image of the EES and BES sites accurately visualized coronary adventitial VV (Figures 4A,D), as was the case in the cross-sectional OFDI image in a pig (Figure 3B). Intriguingly, the magnified OFDI image of the stent edge showed feasibility for manually tracing the adventitial VV area in a patient in vivo (Figure 4A–F). The morphometric analysis showed that the adventitial VV area was significantly greater in the EES site compared with the BES site (Table 4), even after the correction with the adventitial area (calculated as VV area density) (Figure 4G).

Discussion

The major findings of the present study were that: (1) there was a significant positive correlation between adventitial VV area on OFDI and that in histology in the porcine coronary arteries after stent implantation; and (2) OFDI enables us to precisely measure coronary VV area at the stent edge in humans in vivo after stent implantation.

OFDI Measurement of Coronary Adventitial VV

We have recently reported a histological validation demonstrating that adventitial VV on the OFDI images of the human coronary artery accurately correspond to the adventitial VV in histology at human autopsy, and that OFDI is feasible for adventitial VV visualization in the mild coronary lesions in humans in vivo.[15] Although ex vivo micro-computed tomography[24] has been suggested for the volumetric measurement of coronary adventitial VV in pigs, current imaging techniques are still limited to precisely measure coronary adventitial VV area in humans.

Enhanced formation of adventitial VV after coronary stent implantation in pigs[25] and rabbits[26] has been previously demonstrated. Furthermore, we have recently demonstrated that VV neovascularization is prone to extend to the stent edges in the porcine coronary arteries after DES implantation, supplying inflammatory cells/cytokines.[9] In the present study, we thus focused on coronary adventitial VV formation at the stent edges in pigs, demonstrating for the first time that the adventitial VV area at the stent edges on OFDI accurately corresponds to that in histology. The OFDI system has been developed as a new generation of OCT with better image acquisition by removing the depth degeneracy.[27] The minimum area of VV in histology was approximately 500μm^2, and the minimum diameter was 20μm, which are similar to the minimum VV size, as previously reported.[28–30] The resolution of OFDI is at least 20μm.[12] Thus, it is conceivable that the OFDI system can detect the minimal VV detected in histology in the present histological validation study. Such a property of the OFDI technology enables us to precisely measure the signal-voiding tubular structures indicating VV in the coronary adventitia.

Implications of the Present Study

Adventitial inflammation,[1–5] including adventitial VV, plays an important role in the pathogenesis of coronary plaque progression[6,8,10,11] and rupture.[7] Particularly, VV is considered to serve as an outside-in supply route of vascular inflammation.[4] Indeed, it was demonstrated that number of intraplaque microchannels (a part of VV) on OCT is associated with early

manifestation of coronary atherosclerosis in humans in vivo.[21] However, in order to elucidate more precise pathophysiological roles of adventitial VV in humans in vivo, volumetric measurements of adventitial VV area is warranted. In the present study, we were able to measure the adventitial VV area at the stent edges of patients who had undergone coronary stent implantation in vivo. The OFDI system thus should be a promising modality for evaluating coronary adventitial VV. Indeed, in the present study, BES with bioabsorbable polymers was associated with less formation of adventitial VV in the stent edges compared with EES with durable polymers in humans in vivo, suggesting that the OFDI technique is useful to assess the biocompatibility of coronary stents. We have previously demonstrated that chronic adventitial inflammation induces coronary vasospastic activity without impairment of endothelial function in pigs in vivo.[1–3] Further studies with OFDI are needed to examine the involvement of adventitial inflammation and VV formation in the pathogenesis of vasospastic angina.

Interestingly, it was previously demonstrated that prominent VV neovascularization in the coronary adventitia precedes the initiation of coronary lesion formation in hypercholesterolemic pigs.[8] Thus, the inhibition of VV formation by statins[10] and plasminogen activator inhibitor-1,[11] could be a novel therapeutic strategy for CAD. When extrapolating those preclinical findings into the clinical settings, the OFDI system should be useful for examining the effect of anti-angiogenic agents in patients with CAD.

Study Limitations

Several limitations should be mentioned for the present study. First, in the present study, we examined the OFDI images of non-diseased porcine coronary arteries after stent implantation. Thus, it remains to be examined whether OFDI is feasible for adventitial VV measurement in advanced coronary lesions. In such lesions, adventitial VV is likely to develop into the lipid pool, causing an intra-plaque hemorrhage due to its incompetence.[7] In contrast, it has been reported that light sources of OCT are prone to be attenuated at thick atherosclerotic lesions.[31] Second, due to the unavailability of the OFDI system for in vivo experiment with pigs, we performed ex vivo histological validation studies after removal of the porcine heart and subsequent perfusion with saline. Third, it was difficult for us to obtain a clear image of immunohistochemistry for vWF in the resin-embedded stent sections of porcine coronary arteries. In addition, light sources of OFDI are prone to be attenuated at the stent struts. We were thus unable to precisely evaluate adventitial VV area at the stent implantation site. Fourth, because OFDI images were not obtained before stent implantation procedures in pigs or humans in vivo, it remains to be elucidated whether adventitial VV formation is further enhanced after stent implantation in the atherosclerotic plaque with developed VV formation. Finally, it remains to be elucidated whether OFDI is able to identify the nature (arteries vs. veins), the direction (outside-in or inside-out) and functional flow of adventitial VV, all of which are potentially important for fully understanding the roles of adventitial VV in the pathogenesis of CAD.

Conclusions

The present study demonstrates for the first time the accuracy of OFDI for the measurement of coronary adventitial VV in pigs ex vivo and humans in vivo. Thus, the OFDI system is useful to elucidate the roles of coronary adventitial VV in the pathogenesis of CAD in humans.

Acknowledgments

The authors would like to thank Y. Watanabe and A. Nishihara for their excellent technical assistance.

This work was supported, in part, by the grants-in-aid for the Scientific Research (18890018) and the Global COE Project (F02), and the grants-in-aid (H22-Shinkin-004) from the Japanese Ministry of Education, Culture, Sports, Science, and Technology, Tokyo, Japan (to H.S.) and the grant for young investigators of translational research from Tohoku University Hospital (to Y.M.).

Disclosures

Conflicts of Interest: H.S. is a consultant of Asahi Kasei Pharma.

References

1. Shimokawa H, Ito A, Fukumoto Y, Kadokami T, Nakaike R, Sakata M, et al. Chronic treatment with interleukin-1β induces coronary intimal lesions and vasospastic responses in pigs in vivo: The role of platelet-derived growth factor. *J Clin Invest* 1996; **97:** 769–776.
2. Kandabashi T, Shimokawa H, Miyata K, Kunihiro I, Kawano Y, Fukata Y, et al. Inhibition of myosin phosphatase by upregulated Rho-kinase plays a key role for coronary artery spasm in a porcine model with interleukin-1β. *Circulation* 2000; **101:** 1319–1323.
3. Shimokawa H. 2014 Williams Harvey Lecture: Importance of coronary vasomotion abnormalities-from bench to bedside. *Eur Heart J* 2014; **35:** 3180–3193.
4. Maiellaro K, Taylor WR. The role of the adventitia in vascular inflammation. *Cardiovasc Res* 2007; **75:** 640–648.
5. Psaltis PJ, Puranik A, Spoon DB, Chue CD, Hoffman SJ, Witt TA, et al. Characterization of a resident population of adventitial macrophage progenitor cells in postnatal vasculature. *Circ Res* 2014; **115:** 364–375.
6. Barger AC, Beeuwkes R III, Lainey LL, Silverman KJ. Hypothesis: Vasa vasorum and neovascularization of human coronary arteries: A possible role in the pathophysiology of atherosclerosis. *N Engl J Med* 1984; **310:** 175–177.
7. Virmani R, Kolodgie FD, Burke AP, Finn AV, Gold HK, Tulenko TN, et al. Atherosclerotic plaque progression and vulnerability to rupture. *Arterioscler Thromb Vasc Biol* 2005; **25:** 2054–2061.
8. Herrmann J, Lerman LO, Rodriguez-Porcel M, Holmes DR Jr, Richardson DM, Ritman EL, et al. Coronary vasa vasorum neovascularization precedes epicardial endothelial dysfunction in experimental hypercholesterolemia. *Cardiovasc Res* 2001; **51:** 762–766.
9. Nishimiya K, Matsumoto Y, Takahashi J, Uzuka H, Shindo T, Hanawa K, et al. Important role of adventitia in the pathogenesis of coronary hyperconstricting responses after drug-eluting stent implantation in pigs in vivo (abstract). *Circ J* 2014; **78**(Suppl I)**:** I–100.
10. Wilson SH, Herrmann J, Lerman LO, Holmes DR Jr, Napoli C, Ritman EL, et al. Simvastatin preserves the structure of coronary adventitial vasa vasorum in experimental hypercholesterolemia independent of lipid lowering. *Circulation* 2002; **105:** 415–418.
11. Mulligan-Kehoe MJ, Simons M. Vasa vasorum in normal and diseased arteries. *Circulation* 2014; **129:** 2557–2566.
12. Yun SH, Tearney GJ, de Boer JF, Iftimia N, Bouma BE. High-speed optical frequency-domain imaging. *Opt Express* 2003; **22:** 2953–2963.
13. Yun SH, Tearney GJ, Vakoc BJ, Shishkov M, Oh WY, Desjardins AE, et al. Comprehensive volumetric optical microscopy in vivo. *Nat Med* 2006; **12:** 1429–1433.
14. Muramatsu T, Garcia-Garcia HM, Onuma Y, Zhang YJ, Bourantas CV, Diletti R, et al. Intimal flaps detected by optical frequency domain imaging in the proximal segments of native coronary arteries: An innocent bystander? Insights from the TROFI trial. *Circ J* 2013; **77:** 2327–2333.
15. Nishimiya K, Matsumoto Y, Takahashi J, Uzuka H, Odaka Y, Nihei T, et al. In vivo visualization of adventitial vasa vasorum of the human coronary artery on optical frequency domain imaging: Validation study. *Circ J* 2014; **78:** 2516–2518.
16. Shiroto T, Yasuda S, Tsuburaya R, Ito Y, Takahashi J, Ito K, et al. Role of Rho-kinase in the pathogenesis of coronary hyperconstricting responses induced by drug-eluting stents in pigs in vivo. *J Am Coll Cardiol* 2009; **54:** 2321–2329.
17. Tsuburaya R, Yasuda S, Shiroto T, Ito Y, Gao JY, Aizawa K, et al. Long-term treatment with nifedipine suppresses coronary hyperconstricting responses and inflammatory changes induced by paclitaxel-eluting stent in pigs in vivo: Possible involvement of Rho-kinase pathway. *Eur Heart J* 2012; **33:** 791–799.
18. Schwartz RS, Edelman ER, Carter A, Chronos N, Rogers C, Robinson

KA, et al. Drug-eluting stents in preclinical studies: Recommended evaluation from a consensus group. *Circulation* 2002; **106:** 1867–1873.
19. Kwon HM, Sangiorgi G, Ritman EL, Lerman A, McKenna C, Virmani R, et al. Adventitial vasa vasorum in balloon-injured coronary arteries: Visualization and quantitation by a microscopic three-dimensional computed tomography technique. *J Am Coll Cardiol* 1998; **32:** 2072–2079.
20. Tanaka K, Nagata D, Hirata Y, Tabata Y, Nagai R, Sata M. Augmented angiogenesis in adventitia promotes growth of atherosclerotic plaque in apolipoprotein E-deficient mice. *Atherosclerosis* 2011; **215:** 366–373.
21. Choi BJ, Matsuo Y, Aoki T, Kwon TG, Prasad A, Gulati R, et al. Coronary endothelial dysfunction is associated with inflammation and vasa vasorum proliferation in patients with early atherosclerosis. *Arterioscler Thromb Vasc Biol* 2014; **34:** 2473–2477.
22. Murata A, Wallace-Bradely D, Tellez A, Alviar C, Aboodi M, Sheehy A, et al. Accuracy of optical coherence tomography in the evaluation of neointimal coverage after stent implantation. *JACC Cardiovasc Imaging* 2010; **3:** 76–84.
23. Bland JM, Altman DG. Statistical methods for assessing agreement between two methods of clinical measurement. *Lancet* 1986; **1:** 307–310.
24. Ritman EL, Lerman A. The dynamic vasa vasorum. *Cardiovasc Res* 2007; **75:** 649–658.
25. Schwalz RS, Chronos NA, Virmani R. Preclinical restenosis models and drug-eluting stents: Still important, still much to learn. *J Am Coll Cardiol* 2004; **44:** 1373–1385.
26. Sahler LG, Davis D, Saad WE, Patel NC, Lee DE, Waldman DL. Comparison of vasa vasorum after intravascular stent placement with sirolimis drug-eluting and bare metal stents. *J Med Imaging Radiat Oncol* 2008; **52:** 570–575.
27. Yun SH, Tearney GJ, de Boer JF, Bouma BE. Removing the depth-degeneracy in optical frequency domain imaging with frequency shifting. *Opt Express* 2004; **12:** 4822–4828.
28. Komatsu R, Ueda M, Naruko T, Kojima A, Becker AE. Neointimal tissue response at sites of coronary stenting in humans. *Circulation* 1998; **98:** 224–233.
29. Laine P, Kaartinen M, Penttilä A, Panula P, Paavonen T, Kovanen PT. Asscoation between myocardial infarction and the mast cells in the adventitia of the infarct-related coronary artery. *Circulation* 1999; **99:** 361–369.
30. Gössl M, Versari D, Hildebrandt HA, Bajanowski T, Sangiorgi G, Erbel R, et al. Segmental heterogeneity of vasa vasorum neovascularization in human coronary atherosclerosis. *JACC Cardiovasc Imaging* 2010; **3:** 32–40.
31. Kubo T, Tanaka A, Kitabata H, Ino Y, Tanimoto T, Akasaka T. Application of optical coherence tomography in percutaneous coronary intervention. *Circ J* 2012; **76:** 2076–2083.

Supplementary Files

Supplementary File1

Table S1. Procedural parameters of stent implantation in pigs

Table S2. Patient characteristics

Table S3. Intra- and inter-observer variabilities in the OFDI measurement of stent sites

Table S4. Intra- and inter-observer variabilities in the OFDI measurement of stent edges

Table S5. Morphometric analysis of the stent edges with OFDI in pigs

Figure S1. Immunostainings for α-smooth muscle actin (α-SMA) of the stent edge in porcine coronary arteries.

Figure S2. Adventitial vasa vasorum (VV) area on optical frequency domain imaging at the stent edges.

Please find supplementary file(s);
http://dx.doi.org/10.1253/circj.CJ-15-0078